Earth and Planetary Science Letters 557 (2021) 116730

Contents lists available at ScienceDirect

Earth and Planetary Science Letters

www.elsevier.com/locate/epsl

Stirred not shaken; critical evaluation of a proposed Archean meteorite impact in West Greenland

Chris Yakymchuk [a,*], Christopher L. Kirkland [b], Aaron J. Cavosie [c], Kristoffer Szilas [d], Julie Hollis [e], Nicholas J. Gardiner [f], Pedro Waterton [d], Agnete Steenfelt [g], Laure Martin [h]

[a] Department of Earth and Environmental Sciences, University of Waterloo, Canada
[b] Timescales of Mineral Systems Group, Centre for Exploration Targeting - Curtin Node, School of Earth and Planetary Sciences, Curtin University, Perth, Australia
[c] Space Science and Technology Centre, School of Earth and Planetary Sciences, Curtin University, Perth, Australia
[d] Department of Geosciences and Natural Resource Management, University of Copenhagen, Øster Voldgade 10, 1350 Copenhagen K, Denmark
[e] Department of Geology, Ministry of Mineral Resources, Government of Greenland, P.O. Box 930, 3900 Nuuk, Greenland
[f] School of Earth and Environmental Sciences, University of St Andrews, St Andrews, KY16 9AL, United Kingdom
[g] The Geological Survey of Denmark and Greenland, Øster Voldgade 10, 1350 Copenhagen K, Denmark
[h] Centre for Microscopy, Characterisation & Analysis, The University of Western Australia, Perth, Western Australia 6009, Australia

ARTICLE INFO

Article history:
Received 5 November 2020
Received in revised form 16 December 2020
Accepted 18 December 2020
Available online 11 January 2021
Editor: W.B. McKinnon

Keywords:
bolide
impact
Maniitsoq
North Atlantic Craton
planar deformation features
zircon

ABSTRACT

Large meteorite impacts have a profound effect on the Earth's geosphere, atmosphere, hydrosphere and biosphere. It is widely accepted that the early Earth was subject to intense bombardment from 4.5 to 3.8 Ga, yet evidence for subsequent bolide impacts during the Archean Eon (4.0 to 2.5 Ga) is sparse. However, understanding the timing and magnitude of these early events is important, as they may have triggered significant change points to global geochemical cycles. The Maniitsoq region of southern West Greenland has been proposed to record a ~3.0 Ga meteorite impact, which, if confirmed, would be the oldest and only known impact structure to have survived from the Archean. Such an ancient structure would provide the first insight into the style, setting, and possible environmental effects of impact bombardment continuing into the late Archean. Here, using field mapping, geochronology, isotope geochemistry, and electron backscatter diffraction mapping of 5,587 zircon grains from the Maniitsoq region (rock and fluvial sediment samples), we test the hypothesis that the Maniitsoq structure represents Earth's earliest known impact structure. Our comprehensive survey shows that previously proposed impact-related geological features, ranging from microscopic structures at the mineral scale to macroscopic structures at the terrane scale, as well as the age and geochemistry of the rocks in the Maniitsoq region, can be explained through endogenic (non-impact) processes. Despite the higher impact flux, intact craters from the Archean Eon remain elusive on Earth.

1. Introduction

Meteorite impacts have shaped Earth's surface and caused instantaneous changes—some catastrophic—to planetary crusts as well as the atmosphere, oceans, climate and life. Such punctuated violent events are superimposed on gradual geological change (Grey et al., 2003; Schmieder and Kring, 2020). Currently, the oldest confirmed meteorite impact structure formed at 2.23 Ga, and may be associated with the end of global glacial conditions at that time (Erickson et al., 2020). Establishing the timing and size of large and ancient impacts is thus crucial for understanding the development of Earth's surface and the evolution of complex life (Kring, 2000; Osinski et al., 2001; O'Neill et al., 2020). However, most evidence of meteorite impacts on Earth, including the topographic expression of impact craters, becomes progressively removed from the rock record over time through erosion and recycling of crust via normal tectonic processes. For this reason, Archean impact ejecta horizons in South Africa and Australia, which range in age from 3.47 to 2.6 Ga, are currently the oldest evidence of impact processes, yet none have a recognized source crater (Glass and Simonson, 2013). The size of these early impacts, and hence their consequences for Archean Earth systems, are unknown.

The Maniitsoq region of West Greenland has been claimed to host the oldest impact structure on Earth (Garde et al., 2012; Scherstén and Garde, 2013). With a purported age of ~3.00 Ga and a diameter of ~150 km, the Maniitsoq structure is a candi-

* Corresponding author.
E-mail address: cyakymchuk@uwaterloo.ca (C. Yakymchuk).

https://doi.org/10.1016/j.epsl.2020.116730

date source crater for Archean-aged ejecta deposits. The Maniitsoq structure is located in the Archean Akia Terrane of the North Atlantic Craton (Friend et al., 1996; Nutman and Friend, 2007; Polat et al., 2015; Friend and Nutman, 2019). The Akia Terrane is dominated by Mesoarchean gray gneisses (Garde, 1997; Garde et al., 2000) with minor amounts of younger supracrustal rock sequences (Kirkland et al., 2018), variably disrupted ultramafic rock complexes (Szilas et al., 2015), and late-tectonic felsic to mafic igneous intrusions (Fig. 1). A broadly arcuate array of mafic rocks in the region (Fig. 1) was proposed to represent mantle-derived melt produced by a 3.0 Ga bolide impact (Garde et al., 2012, 2013). Published U–Pb zircon ages in five granitoid rocks cluster around 3.00 Ga; their isotope systematics were interpreted as evidence for an impact-induced hydrothermal overprint, and regarded as the minimum age of that impact event (Scherstén and Garde, 2013). Other evidence that has been put forward in support the Maniitsoq impact hypothesis includes mineral microstructures interpreted to have formed during high-strain (shock) deformation, putative impact melt, curvilinear aeromagnetic anomalies, rock brecciation, and platinum group element abundances (Garde et al., 2012, 2013, 2014; Scherstén and Garde, 2013; Keulen et al., 2015). Of these, only deformation microstructures in minerals provide diagnostic evidence of impact processes (French and Koeberl, 2010) and the data presented of alleged shocked quartz from Maniitsoq rocks has been challenged (Reimold et al., 2013). Given that the preservation potential for Archean impact structures is low (none are currently known), it is crucial to investigate materials at Maniitsoq that can provide unambiguous evidence of shock metamorphism in deep crustal rocks, such as shock microstructures in the refractory mineral zircon (Kamo et al., 1996; Moser et al., 2011; Timms et al., 2017), rather than quartz and feldspar, where evidence of impact deformation can more easily anneal over geologic time (French and Koeberl, 2010).

We evaluate the hypothesis that the Maniitsoq structure represents an Archean-age impact crater that formed ca. 3 Ga by integrating new field observations, geochronology, isotope geochemistry, and a microstructural survey of 2,256 zircon grains from 18 basement rocks and 3,331 zircon grains from 14 stream sediments from across the Maniitsoq region (Fig. 1). Field observations and geochronology of key samples from the central area of the proposed Maniitsoq structure are used to determine the timing of magma crystallization and regional deformation. Electron backscatter diffraction imaging is used to investigate if zircon from throughout the Maniitsoq structure shows evidence of shock metamorphism and is coupled with an expansive study of detrital grains in fluvial systems from nearby drainages. Finally, oxygen isotope geochemistry of zircon evaluates the proposal that bolide impact caused an influx of surface waters in rocks exposed in the Maniitsoq region.

2. Materials and methods

2.1. Rock and mineral samples

Two granitoid samples previously proposed to be impact-generated melts that formed at 3.0 Ga (Garde et al., 2012; Keulen et al., 2015) were collected for U–Pb zircon geochronology and O isotope analysis and complement 15 additional bedrock samples with published U–Pb zircon ages (Fig. 1; Supplementary Table S1). Of these existing 15 samples, seven have crystallization ages >3.0 Ga, six have crystallization ages <3.0 Ga, and two are metasedimentary rocks with depositional ages < 3.0 Ga (Supplementary Table S1). An additional sample (a metaleucogabbro; sample 488) was also analyzed to relate its crystallization age to microstructures measured with electron backscatter diffraction (EBSD). Together, this set of 18 bedrock samples provides a balance of zircon that is both older and younger than the proposed age (~3.0 Ga) of impact at Maniitsoq. An additional 3,331 zircon grains from 14 stream sediment samples representing various drainages across the terrane (Fig. 1) were also surveyed for EBSD as a means of expanding regional bedrock sampling of rocks that may be poorly exposed or no longer extant.

The first proposed impact-related sample is an alkali-feldspar-rich pegmatite (sample 899; Fig. 2a) from the Maniitsoq structure (Fig. 1), consistent with those described previously as the product of impact-induced melting (Garde et al., 2012). The pegmatite contains cm-sized alkali-feldspar porphyroclasts (Fig. 2a) which implies substantial ductile deformation after crystallization.

A second rock proposed to be related to impact-induced melting is an equigranular felsic gneiss (sample 1240) that was sampled near the location where microstructural evidence of impact melt was proposed (Keulen et al., 2015). The equigranular felsic gneiss is folded with the enveloping mafic gneiss (Fig. 2b).

2.2. U–Pb zircon geochronology.

Zircon geochronology was conducted using a Resonetics RESOlution M–50A–LR laser ablation system, incorporating a COMPex 102 193 nm excimer UV laser coupled to a Nu Plasma II multi-collector inductively coupled plasma mass spectrometer. Detailed analytical methods are presented in Appendix A in the supplementary material.

2.3. O isotope analysis in zircon

Oxygen isotope ratios and $^{16}O^{1}H/^{16}O$ (OH^{-}) values were determined on new and previously dated zircon grains using a Cameca IMS 1280 at the Centre for Microscopy Characterisation and Analysis at the University of Western Australia. Analytical procedures closely followed those of Kita et al. (2009) and the data reduction follows protocols described previously by Kirkland et al. (2012). Detailed analytical methods are found in Appendix A.

2.4. Electron backscatter diffraction

Zircon grains from 18 rock samples (2,256 grains) and 14 stream sediment samples (3,331 grains) collected across the Maniitsoq region (Fig. 1) were surveyed for deformation by electron backscatter diffraction (EBSD). Zircon grains were mounted in epoxy resin, and some are the same samples that were analyzed for U–Pb geochronology and oxygen isotope ratios. Scanning electron microscopy (SEM) analysis was performed using a Tescan MIRA3 field emission gun (FEG) SEM in the Microscopy and Microanalysis Facility in the John de Laeter Centre at Curtin University using methods described previously (e.g., Cavosie et al., 2018). Details of sample preparation and instrument operating conditions are presented in Appendix A in the supplementary material.

3. Results

3.1. Field relationships

New geologic mapping conducted during field campaigns in 2016–2018 has identified a polyphase deformation history in the Maniitsoq region that builds on, and is consistent with, previous interpretations (Garde et al., 2000; Kirkland et al., 2018; Berthelsen, 1962; Steenfelt et al., 2020). Here, we present a brief summary of the field observations with further details found in Kirkland et al. (2018) and Steenfelt et al. (2020).

The earliest fabric is preserved in mafic enclaves and this fabric is folded into locally-preserved and variably-oriented folds. The

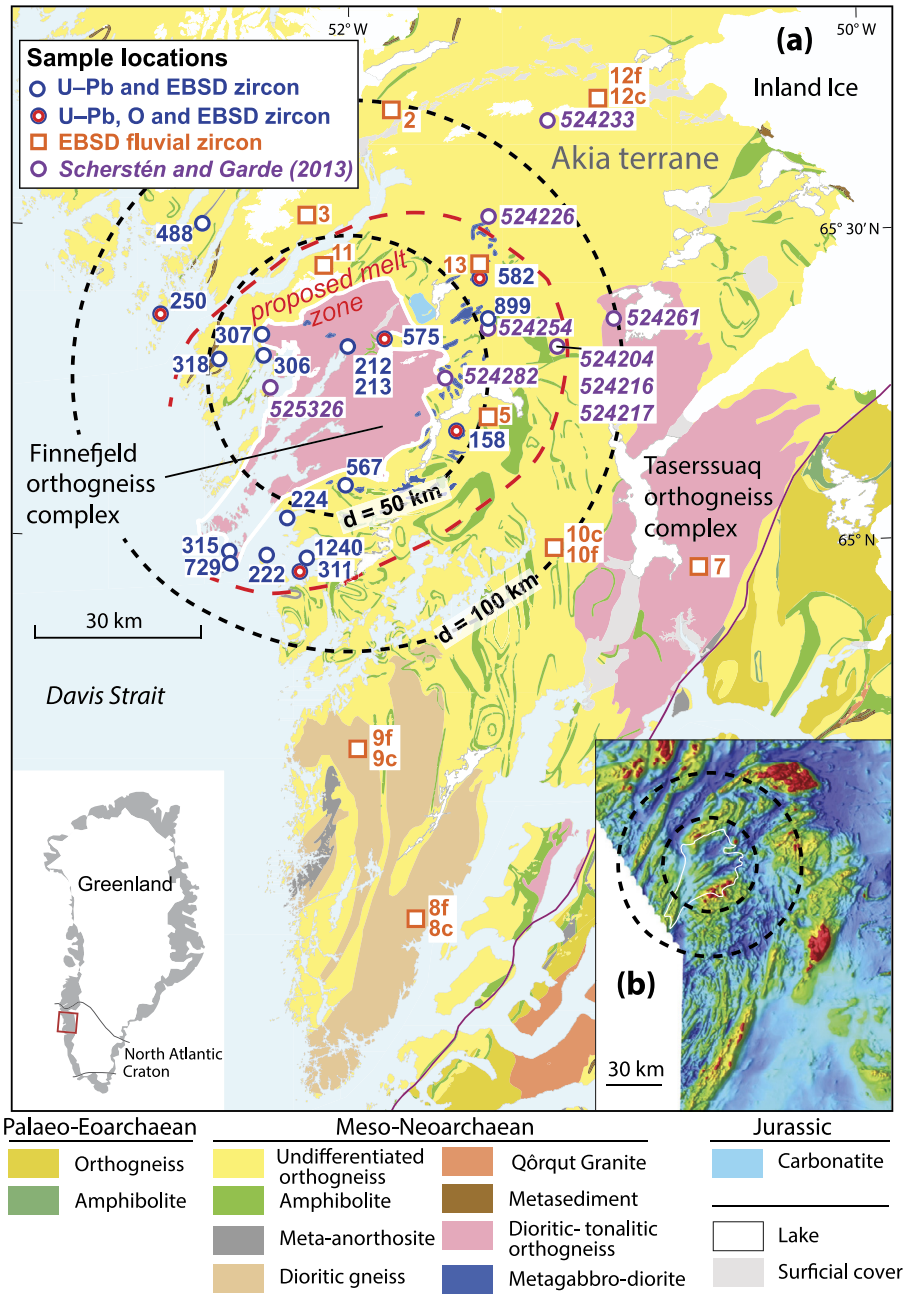

Fig. 1. (a) Geological map of the Akia Terrane of the North Atlantic Craton, southern West Greenland (map modified from Allaart, 1982 and Gardiner et al., 2019). Dashed red line indicates the inferred location of the melt zone associated with the proposed Maniitsoq impact structure (Garde et al., 2012). Dashed black lines show the proposed distance from the center of the impact crater (Garde et al., 2012; Scherstén and Garde, 2013). Samples from Scherstén and Garde (2013) were used to argue for pervasive isotopic resetting of zircon at 3.0 Ga due to a bolide impact. (b) Aeromagnetic map of the Akia Terrane and surroundings, illustrating regionally developed fold patterns that developed after 3.0 Ga (modified from Steenfelt et al., 2020). The spatial extent of map is the same as in (a). Sources of data for each sample are detailed in the Supplementary Tables. (For interpretation of the colors in the figure(s), the reader is referred to the web version of this article.)

age of this early fabric is unclear, but it is younger than the crystallization age of diorite gneiss that hosts this fabric (dated at 3.2 Ga; Garde et al., 2000) and older than the enveloping tonalite (>3.0 Ga; Garde et al., 2000; Gardiner et al., 2019). A second-generation fabric forms the dominant gneissosity in the tonalites, and is isoclinally folded at the outcrop- to map scale. The dominant regional tectonic fabric (Fig. 1b) is a third-generation foliation that is parallel to the contacts between the supracrustal rocks and the enveloping tonalite gneiss (Fig. 1a) and present as foliations in metabasites and metasedimentary rocks. Second and third-generation structures are associated with high-temperature metamorphism at <2.88 Ga (Kirkland et al., 2018).

3.2. Zircon geochronology

U–Pb analytical data are presented in Supplementary Table S2. The results for sample 488 (metaleucogabbro) are described in detail in Appendix B in the supplementary material.

3.2.1. Sample 899

Zircon crystals are dominantly euhedral, many are brown to black, implying high to extreme U content. There is some morphological variation within the grains (Fig. 3a); most have well-defined crystal faces, some are angular broken fragments, and some are rounded. Under CL imaging many grains reveal idiomorphic zoning

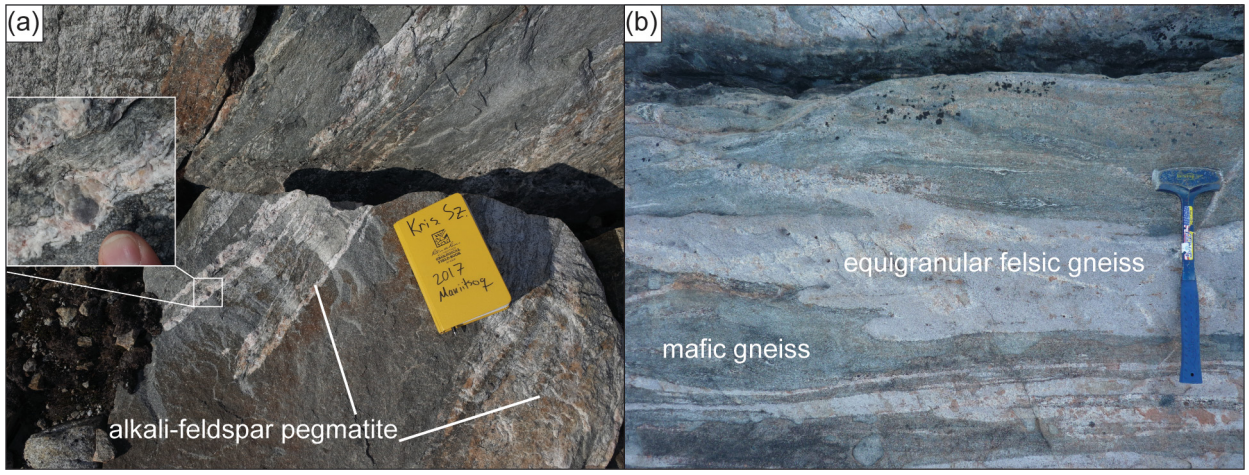

Fig. 2. (a) Alkali-feldspar pegmatite (sample 899). Porphyroclasts of alkali-feldspar (inset) indicate significant subsolidus ductile deformation. Sample location: 65.35302° N, 51.44110° W. (b) Equigranular felsic gneiss (similar to sample 1240) folded with enveloping mafic gneiss. Photo location: 64.96659° N, 52.13032° W.

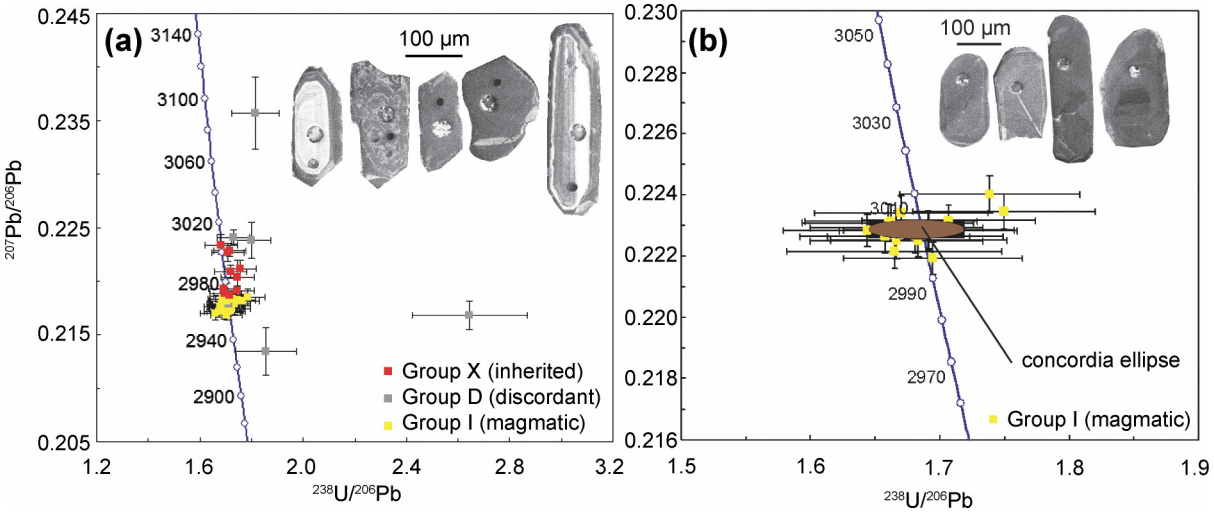

Fig. 3. (a) U–Pb analytical data for zircons from sample 899: alkali-feldspar pegmatite. Yellow squares indicate Group I (magmatic zircon); red squares indicate Group X (inherited zircon); gray squares indicate Group D (discordant or high common Pb). (b) U–Pb analytical data for zircons from sample 1240: equigranular gneiss. Yellow squares indicate Group I (magmatic zircon). Concordia ellipse is shown in brown.

whereas a few grains are traversed by a network of fractures. These fractures are cored by low CL response zircon but edged by high CL response zircon. Some grains have a spongy texture. A total of 46 analyses were made on 46 grains. Six analyses have greater than 2% non-radiogenic lead as determined using the ^{204}Pb approach or are >5% discordant (Fig. 3a). These six analyses (Group D) are interpreted to have lost or gained Pb, including potentially non-radiogenic Pb, and are excluded from further discussion. Thirty analyses (Group I), on homogeneous domains in oscillatory zoned zircon yield a $^{207}Pb/^{206}Pb$ weighted mean age of 2963 ± 1 Ma (MSWD = 2.2), interpreted as the age of high-grade metamorphism and melting. Group I grains have high concentrations of U (average 598 ppm) and moderate Th/U ratios (average 0.91). Ten analyses (Group X) on CL-bright cores yield $^{207}Pb/^{206}Pb$ ages of 3005–2971 Ma, interpreted as either the age of xenocrystic components or dates reflecting variable degrees of radiogenic Pb loss from a ca. 3.0 Ga component during overprinting at ca. 2960 Ma. Group X has highly variable Th/U ratios, potentially consistent with more than one inherited source, but, in general, their Th/U ratios are very high (2.6 to 0.56, with an extreme outlier at 11.4). Calculated densities, assuming annealing stopped at crystallization, are low for Group I reflecting high to extreme U and Th content (average = 4.15 g/cc), in contrast Group X has higher apparent densities (average = 4.3 g/cc).

3.2.2. Sample 1240

Zircon crystals are subhedral to euhedral, with somewhat rounded terminations. There is very little morphological variation, and under CL most grains display a relatively homogeneous low response with faint indications of oscillatory zoning (Fig. 3b). Some grains have convoluted internal textures consistent with some form of dissolution and subsequent new growth process. A total of 16 analyses were made on 16 grains (Fig. 3b). All sixteen analyses (Group I) yield a Concordia age of 3002 ± 1 Ma (MSWD = 1.9 concordance and equivalence), interpreted as the age of magmatic crystallization. Uranium content is moderate (average 270 ppm) and the Th/U ratio is relatively low (average 0.5). Calculated apparent densities range from 4.6 to 4.3 g/cc, assuming damage accumulation commencing after growth, consistent with Archean zircon and intermediate levels of alpha dose damage.

3.3. Zircon microstructural survey

A total of 2,256 zircon grains from 18 rock samples within the inner 100 km diameter of the proposed impact structure (Fig. 1a)

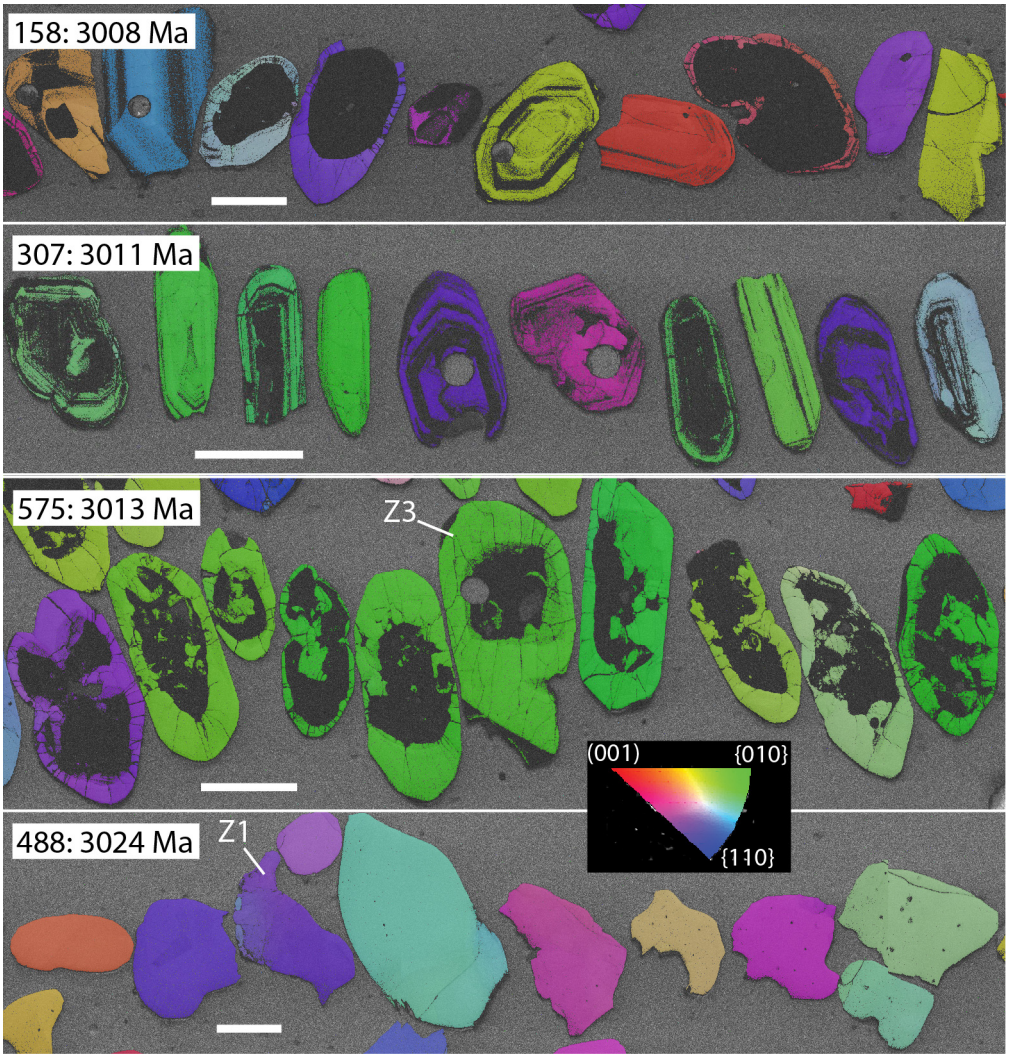

Fig. 4. Electron backscatter diffraction orientation maps (inverse pole figures) of representative zircon grains in Maniitsoq granitoid samples ranging in age from 3024 to 3008 Ma. Colors indicate crystallographic orientation; deformation would manifest as color variations in single grains. Dark areas are metamict (radiation damaged) portions of zircon grains that are no longer crystalline. Circular holes are areas analyzed for U–Pb geochronology by laser ablation inductively coupled mass spectrometry. Scale bars are all 100 micrometers. The pixel size for each image is 500 nm.

were surveyed for deformation using electron backscatter diffraction. These include nine granitoid samples with crystallization ages of 3240–3002 Ma that predate the proposed impact event, seven granitoid samples with crystallization ages of 2998–2729 Ma that postdate the putative impact, and two metasedimentary rocks with depositional ages <3000 Ma (Supplementary Table S1). Fifty-two to 283 zircons per sample were analyzed (average of 125 grains/rock sample; Supplementary Table S4). In addition, 14 fluvial sediment samples were analyzed with 119 to 319 zircons per sample (average of 238 grains/fluvial sample) for a total of 3,331 grains (Supplementary Table S5).

Across the entire zircon suite (5,587 grains), most grains yield high-quality diffraction patterns, in whole or part, indicating zircon across the region is predominantly crystalline. Exceptions at the grain-scale include discrete zones or bands of radiation damage caused by locally high actinide abundances, which are common in zircon (e.g. Nasdala et al., 2005). Radiation damaged areas lose crystallinity and do not generate diffraction patterns, and thus appear black in orientation maps (Fig. 4). Nearly all grains analyzed preserve evidence of oscillatory growth zoning, typically manifested in cores or rims, consistent with an igneous origin (Fig. 4). Some grains show minor evidence of brittle deformation in the form of irregular fractures that are typical for zircon in exhumed plutonic rocks. However, none of the analyzed zircon grains contain sets of parallel planar fractures that are typical of impact-related deformation (e.g. Cavosie et al., 2010).

3.4. Oxygen isotope ratios in zircon

We analyzed O isotope values and OH contents for zircon grains from five samples located within the central 100 km diameter region of the Maniitsoq structure (Fig. 1). Thirty zircon analyses with primary signatures (i.e. low $^{16}O^{1}H/^{16}O$) yield $\delta^{18}O$ values ranging from 5.0 ± 0.4 to 7.0 ± 0.4‰ relative to Vienna Standard Mean Ocean Water (VSMOW) (Fig. 5a). All but six analyses on the zircon grains have low $^{16}O^{1}H/^{16}O$ values within the range of the zircon U–Pb standards (Fig. 5b).

4. Discussion

4.1. Geochronology

An alkali-feldspar-rich pegmatite (sample 899) is from the core of the Maniitsoq structure and similar samples were inferred to be generated from impact-induced melting (Garde et al., 2012). The weighted mean age of 2.963 ± 0.001 Ga from sample 899

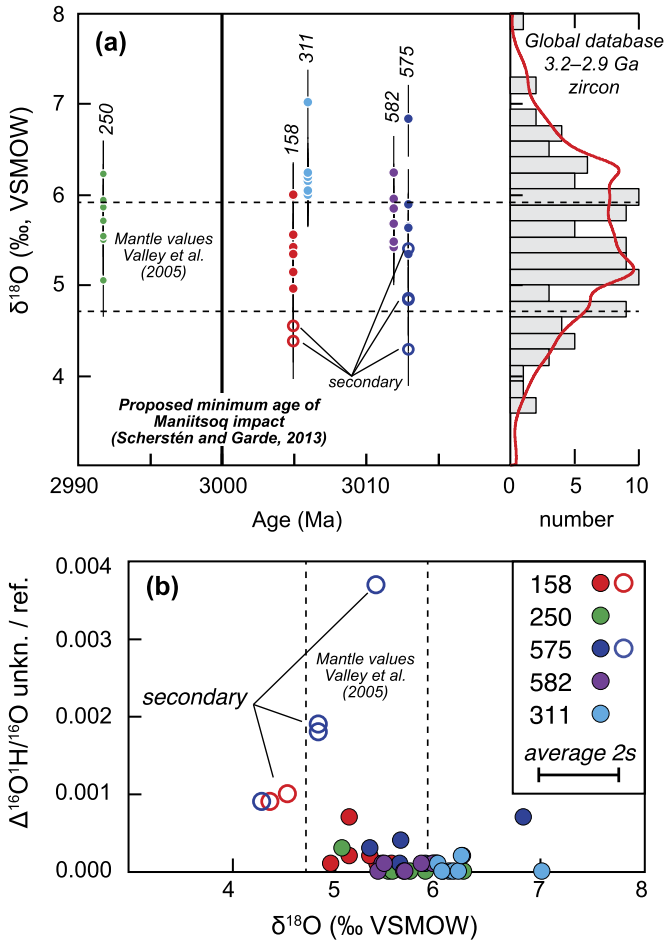

Fig. 5. Stable isotope ratios in zircon. (a) δ^{18}O values of zircon from Maniitsoq rocks. Four samples have crystallization ages older than the proposed impact and would have been affected by the putative impact event. All measured values are inconsistent with the incorporation of surface water (<0‰, VSMOW). The range of global 3.2–2.9 Ga zircon oxygen isotope ratios from primitive crust is from Valley et al. (2005) and Spencer et al. (2014). (b) $^{16}O^{1}H/^{16}O$ of Maniitsoq zircon (unkn.) relative to the reference material (ref.) indicating minimal evidence for secondary alteration. Open symbols are from metamict (radiation damaged) areas of grains and are indicative of alteration; these analyses yield similar δ^{18}O values to unaltered grains (filled symbols).

is interpreted as the age of high-grade metamorphism and melt crystallization based on analyses in homogeneous domains in oscillatory zoned zircon (e.g. Rubatto, 2017). This age is too young to have been generated from the proposed 3.0009 ± 0.0019 Ga minimum age of impact (Scherstén and Garde, 2013), but is generally consistent with recent studies that demonstrate prolonged magmatism and high-temperature metamorphism affected the Akia terrane from ca. 3.05 to 2.97 Ga (Gardiner et al., 2019; Steenfelt et al., 2020). Furthermore, protracted magmatism and metamorphism over ca. 80 Ma is not consistent with an impact, which is a relatively short-lived thermal event.

An equigranular gneiss (our sample 1240) that was previously described as containing impact-related melt microstructures (Keulen et al., 2015) yielded a crystallization age of 3.002 ± 0.001 Ga. This gneiss is intercalated with previously dated younger supracrustal rocks, which suggests younger interleaving and folding at granulite-facies conditions (Kirkland et al., 2018). Pervasive folding of this unit after crystallization reflects the previously documented polyphase deformation history that must have occurred after 3.0 Ga (Kirkland et al., 2018); thus, a circular 3.0 Ga impact-related structure would not be preserved. Hence, based on the temporal relationship of fabrics, an impact crater formed as a circular feature at ca. 3.0 Ga could not be preserved as such in the Maniitsoq region, due to younger pervasive polyphase ductile deformation. Even modest amounts of strain would modify the shape of an originally circular structure in the crust (e.g. Riller, 2005). Furthermore, aeromagnetic data do not support the presence of a circular structure in the Maniitsoq region (Steenfelt et al., 2020).

4.2. Zircon microstructure

Shock-deformation microstructures in zircon provide diagnostic evidence of impact (Timms et al., 2017), and can survive post-impact high-temperature metamorphism in the deep crust (Erickson et al., 2020; Moser et al., 2011) as well as magmatic recycling (Gibson et al., 1997). In general, the vast majority (99.9%) of our comprehensive suite of 5,587 zircons surveyed from the Maniitsoq region record no deformation. Less than ten zircon grains were identified that show evidence of crystal-plastic deformation, which manifests as crystallographic misorientation; cumulative misorientation per grain was ≪5° in all but three grains analyzed. Bedrock samples that contain deformed grains include sample 311 (1 of 114 grains), located >50 km southwest of the center of the Maniitsoq structure, sample 488 (2 of 98 grains), located ~80 km northeast of the center (Fig. 1), and detrital samples 9, 12, and 13 (three grains) (Fig. 6). Deformation in these grains manifests as systems of sub-parallel low-angle grain boundaries, resulting in progressive cumulative misorientation of up to ~10° across each grain (Fig. 6a,c,d), as well as localized recrystallization (Fig. 6b). These types of microstructure are typical of endogenic deformation in shear zones or other discrete high-strain environments, and have been reported in zircon from both tectonic and magmatic settings (Reddy et al., 2009; Piazolo et al., 2012). The microstructures in detrital zircon from across the Maniitsoq region are similar to that observed in bedrock (Fig. 6), and provide a robust verification that no deformed bedrock units were omitted in our sample suite.

Zircon from across the Maniitsoq region record no evidence of high-pressure shock deformation, such as deformation twin lamellae or high-pressure minerals, as has been found in zircon at many of Earth's ~190 confirmed impact structures (Earth Earth Impact Database, 2020). Moreover, the highly crystalline nature and preservation of igneous growth zoning in most of the investigated zircon grains is inconsistent with recrystallization due to a pervasive regional hydrothermal alteration event proposed to have shortly followed impact (cf. Scherstén and Garde, 2013).

4.3. Oxygen isotopes

Meteorite impacts can cause widespread hydrothermal alteration (Osinski et al., 2013) and the geochemical imprint can be evaluated using stable isotopes (Muttik et al., 2010). Scherstén and Garde (2013) propose pervasive and nearly complete isotopic resetting of Maniitsoq zircon during a regional hydrothermal event associated with impact at 3.0009 ± 0.0019 Ga. The hydrothermal alteration process was proposed to have involved dissolution–reprecipitation of zircon, resulting in near-complete expulsion of radiogenic-Pb from the zircon grains at that time.

The oxygen isotope ratio (δ^{18}O) in zircon is a sensitive indicator of both primary growth and/or secondary alteration processes. Mantle-equilibrated zircon has a narrow range of δ^{18}O values of 5.3 ± 0.6‰ (VSMOW); high and low-temperature water–rock interaction, and melting of supracrustal material (δ^{18}O > ~6.5‰ VSMOW) all impart distinctive isotopic signatures on zircon (Valley et al., 2005).

Our δ^{18}O analyses are within uncertainty or higher than values for zircon derived from the mantle (Fig. 5a; Valley et al., 2005) and hence inconsistent with that expected for zircon grown or re-

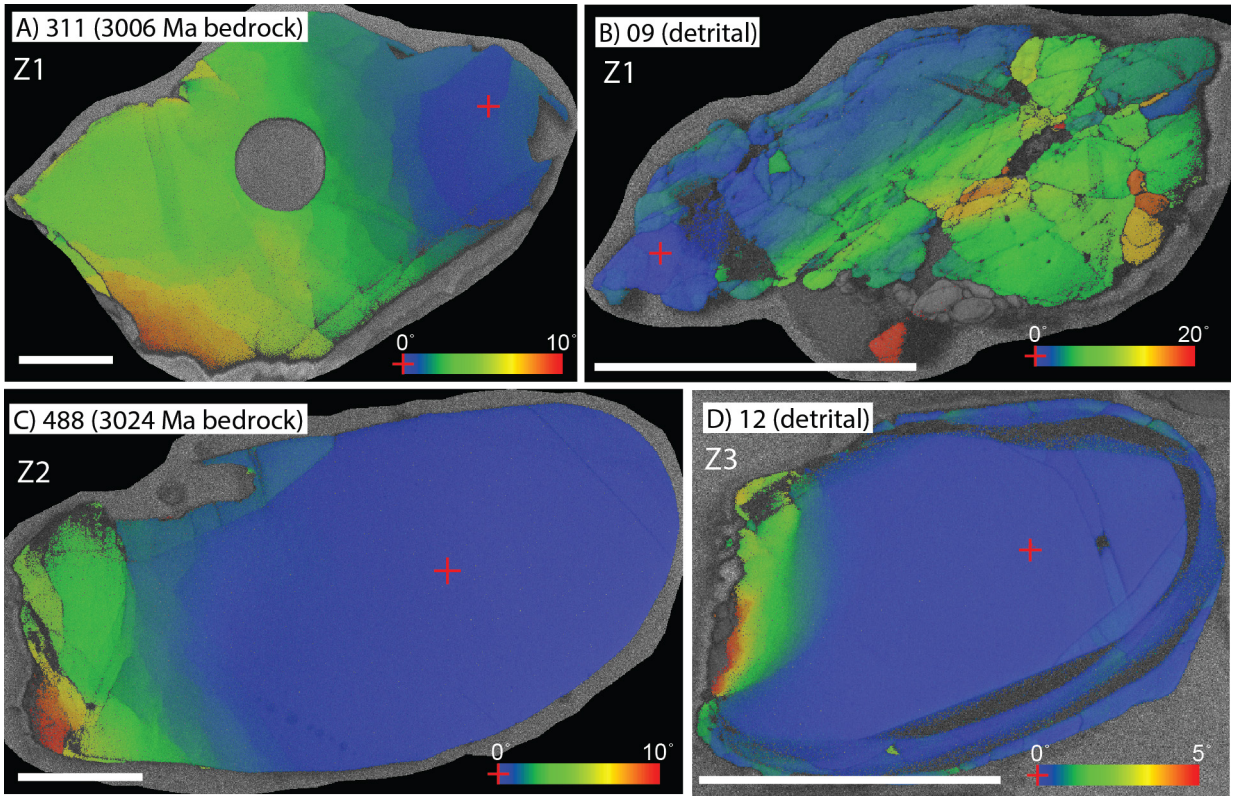

Fig. 6. Electron backscatter diffraction orientation maps showing crystallographic misorientation of zircon grains with crystal-plastic deformation from Maniitsoq samples (sample locations in Fig. 1a). Each of the grains records up to ~10° of misorientation that is accommodated by a system of sub-parallel low-angle grain boundaries, and in the case of (B), localized recrystallization – these styles of deformation in zircon are consistent with tectonic and magmatic processes. The circular feature in (A) is a hole made during the U–Pb analysis by laser ablation. Scale bars are 50 micrometers in length. The pixel sizes for these images range from 150 to 300 nm.

precipitated in a reservoir buffered by Archean seawater (<0‰ relative to VSMOW; Jaffrés et al., 2007).

An additional test for aqueous alteration of zircon, which has been shown to affect primary $\delta^{18}O$ values, is *in situ* measurement of $^{16}O^{1}H/^{16}O$ (Wang et al., 2014). The low $^{16}O^{1}H/^{16}O$ values of all but six spot analyses (Fig. 5b) unambiguously demonstrate that Maniitsoq zircon grains were not aqueously altered or recrystallized in a water-rich environment (e.g. Van Kranendonk et al., 2015). Those six analyses from 42 grains with elevated $^{16}O^{1}H/^{16}O$ values are consistent with the incorporation of H_2O during secondary processes in metamict (radiation-damaged) zircon; such zircon domains are easily identified from their modified U/Pb systematics (indicating radiogenic Pb mobility), as well as identified as dark (non-crystalline) areas in electron backscatter diffraction orientation maps (see sample 575 grain Z3 in Figs. 2 and 7).

Metamict zircon occurs widely in Archean rocks primarily due to accumulated unannealed radiation damage, which allows incorporation of H_2O into the damaged zircon structure environment (Van Kranendonk et al., 2015). Regardless, their $\delta^{18}O$ values (4.3 ± 0.4 to 5.4 ± 0.4‰) are similar to the mantle range (Bindeman, 2008) and of 3.2–2.9 Ga zircon derived from primitive crust globally (Fig. 5a) (Valley et al., 2005; Spencer et al., 2014), and are inconsistent with alteration or recrystallization in a seawater-rich environment. Therefore, there is no stable isotopic evidence in zircon from the Maniitsoq structure that supports a hydrothermal influx of seawater, from bolide impact or other processes.

5. Conclusions

The timing of fabric development, the absence of impact-related microstructures in zircon, and the primary oxygen isotope ratios of zircon all repudiate the hypothesis that the Maniitsoq structure in southern West Greenland formed as a consequence of meteorite impact and related processes at ca. 3.0 Ga. To date, no diagnostic evidence of impact-related deformation has been presented, and moreover, the geologic features in the area are consistent with existing models of regional endogenic processes during polyphase magmatism, tectonism and metamorphism associated with Mesoarchean to Neoarchean growth, reworking and stabilization of the North Atlantic Craton. Our results conclusively rule out the proposal that much of the Archean rock mass in the Maniitsoq region formed by an Archean meteorite impact, which leaves the 2.23 Ga Yarrabubba structure in Western Australia as the oldest confirmed terrestrial impact structure. The source craters for Archean-aged impact ejecta remain elusive on Earth.

CRediT authorship contribution statement

Chris Yakymchuk: Conceptualization, Investigation, Writing – original draft, Writing – review & editing. **Christopher L. Kirkland:** Conceptualization, Formal analysis, Investigation, Methodology, Writing – review & editing. **Aaron J. Cavosie:** Formal analysis, Investigation, Methodology, Writing – review & editing. **Kristoffer Szilas:** Conceptualization, Investigation, Writing – original draft, Writing – review & editing. **Julie Hollis:** Conceptualization, Investigation, Writing – review & editing. **Nicholas J. Gardiner:** Investigation, Writing – review & editing. **Pedro Waterton:** Investigation, Writing – review & editing. **Agnete Steenfelt:** Investigation, Writing – review & editing. **Laure Martin:** Formal analysis.

Declaration of competing interest

The authors declare that they have no known competing financial interests or personal relationships that could have appeared to influence the work reported in this paper.

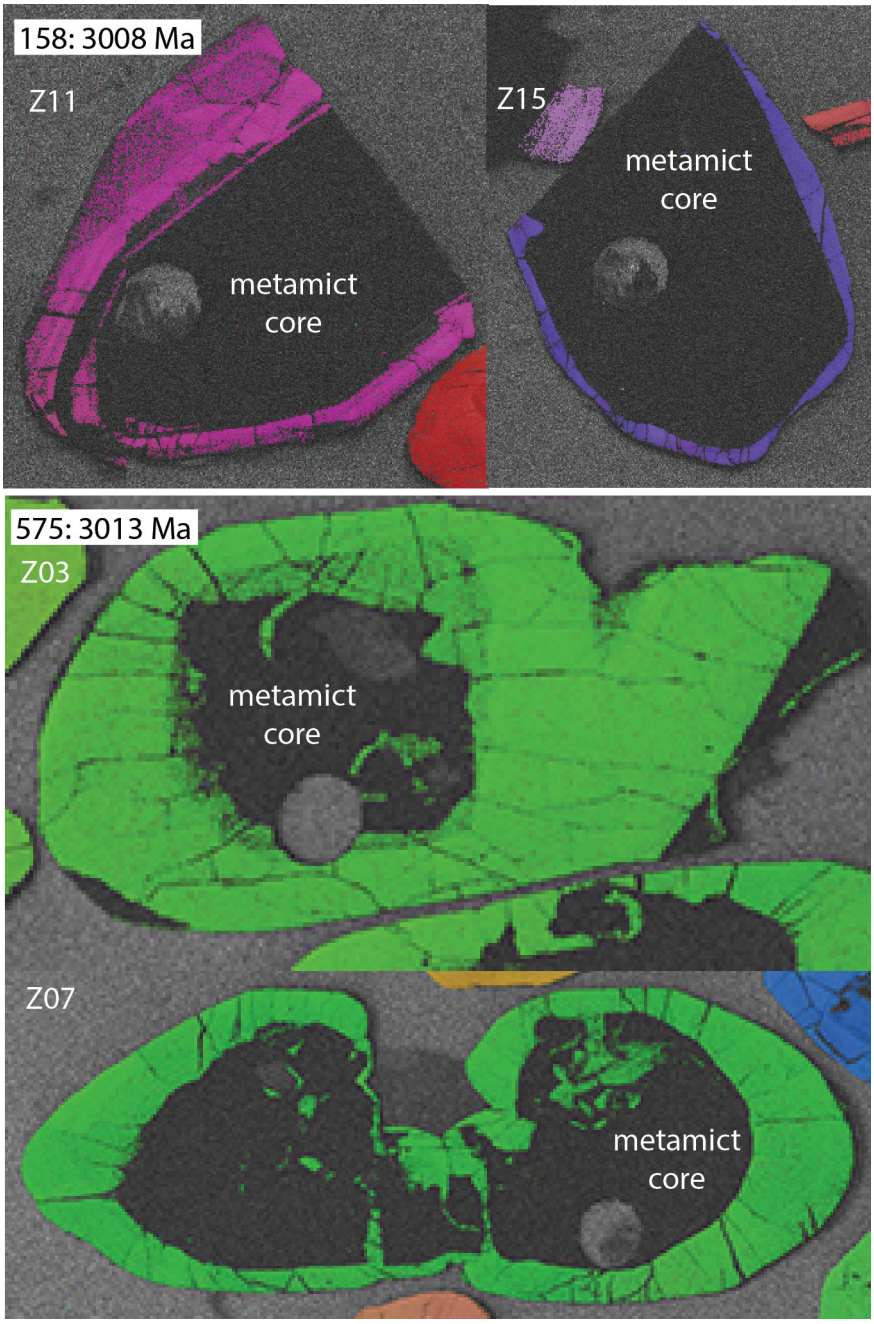

Fig. 7. Electron backscatter diffraction images (inverse pole figures) of high OHO grains showing the metamict nature of the analyzed regions. The same color legend in Fig. 4 applies to this image. The pixel size for each image is 500 nm.

Acknowledgements

The Ministry of Mineral Resources and Labour, Greenland Government supported field and analytical work. We thank John Spray and Christian Koeberl for constructive reviews and William McKinnon for editorial handling.

Appendix. Supplementary material

Supplementary material related to this article can be found online at https://doi.org/10.1016/j.epsl.2020.116730.

References

Allaart, J.H., 1982. Geologisk kort over Grønland, 1:500 000, Sheet 2 Frederikshåb Isblink - Søndre Strømfjord. Grønlands Geologiske Undersøgelse, Copenhagen.

Berthelsen, A., 1962. Structural studies on the pre-Cambrian of western Greenland III. Southern Sukkertoppen district. Bull. Gronlands Geol. Undersogelse 31. 47 p.

Bindeman, I., 2008. Oxygen isotopes in mantle and crustal magmas as revealed by single crystal analysis. Rev. Mineral. Geochem. 69, 445–478.

Cavosie, A.J., Quintero, R.R., Radovan, H.A., Moser, D.E., 2010. A record of ancient cataclysm in modern sand: shock microstructures in detrital minerals from the Vaal River, Vredefort Dome, South Africa. Geol. Soc. Am. Bull. 122, 1968–1980.

Cavosie, A.J., Timms, N.E., Ferrière, L., Rochette, P., 2018. FRIGN zircon—the only terrestrial mineral diagnostic of high-pressure and high-temperature shock deformation. Geology 46, 891–894.

Earth Impact Database, 2020. http://www.passc.net/EarthImpactDatabase. (Accessed 4 November 2020).

Erickson, T.M., Kirkland, C.L., Timms, N.E., Cavosie, A.J., Davison, T.M., 2020. Precise radiometric age establishes Yarrabubba, Western Australia, as Earth's oldest recognised meteorite impact structure. Nat. Commun. 11, 300.

French, B.M., Koeberl, C., 2010. The convincing identification of terrestrial meteorite impact structures: what works, what doesn't, and why. Earth-Sci. Rev. 98, 123–170.

Friend, C.R.L., Nutman, A.P., 2019. Tectono-stratigraphic terranes in Archaean gneiss complexes as evidence for plate tectonics: the Nuuk region, southern West Greenland. Gondwana Res. 72, 213–237.
Friend, C., Nutman, A.P., Baadsgaard, H., Kinny, P.D., McGregor, V.R., 1996. Timing of late Archaean terrane assembly, crustal thickening and granite emplacement in the Nuuk region, southern West Greenland. Earth Planet. Sci. Lett. 142, 353–365.
Garde, A.A., 1997. Accretion and evolution of an Archaean high-grade grey gneiss–amphibolite complex: the Fiskefjord area, southern West Greenland. Geol. Greenland Surv. Bull. 177. 115 p.
Garde, A.A., Friend, C.R.L., Nutman, A.P., Marker, M., 2000. Rapid maturation and stabilisation of middle Archaean continental crust: the Akia terrane, Southern West Greenland. Bull. Geol. Soc. Denmark 47, 1–27.
Garde, A.A., Dyck, B., Esbensen, K.H., Johansson, L., Moller, C., 2014. The Finnefjeld domain, Maniitsoq structure, West Greenland: differential rheological features and mechanical homogenisation in response to impacting? Precambrian Res. 255, 791–808.
Garde, A.A., McDonald, I., Dyck, B., Keulen, N., 2012. Searching for giant, ancient impact structures on Earth: the Mesoarchaean Maniitsoq structure, West Greenland. Earth Planet. Sci. Lett. 337, 197–210.
Garde, A.A., Pattison, J., Kokfelt, T.F., McDonald, I., Secher, K., 2013. The norite belt in the Mesoarchaean Maniitsoq structure, southern West Greenland: conduit-type Ni-Cu mineralisation in impact-triggered, mantle-derived intrusions? Geol. Surv. Denmark Greenland Bull., 45–48.
Gardiner, N.J., Kirkland, C.L., Hollis, J., Szilas, K., Steenfelt, A., Yakymchuk, C., Heide-Jørgensen, H., 2019. Building Mesoarchaean crust upon Eoarchaean roots: the Akia Terrane, West Greenland. Contrib. Mineral. Petrol. 174, 20.
Gibson, R.L., Armstrong, R.A., Reimold, W.U., 1997. The age and thermal evolution of the Vredefort impact structure: a single-grain U-Pb zircon study. Geochim. Cosmochim. Acta 61, 1531–1540.
Glass, B.P., Simonson, B.M., 2013. Distal Impact Ejecta Layers: Impact Studies. Springer, Berlin. 716 p.
Grey, K., Walter, M.R., Calver, C.R., 2003. Neoproterozoic biotic diversification: Snowball Earth or aftermath of the Acraman impact? Geology 31, 459–462.
Jaffrés, J.B., Shields, G.A., Wallmann, K., 2007. The oxygen isotope evolution of seawater: a critical review of a long-standing controversy and an improved geological water cycle model for the past 3.4 billion years. Earth-Sci. Rev. 83, 83–122.
Kamo, S.L., Reimold, W.U., Krogh, T.E., Colliston, W.P., 1996. A 2.023 Ga age for the Vredefort impact event and a first report of shock metamorphosed zircons in pseudotachylitic breccias and granophyre. Earth Planet. Sci. Lett. 144, 369–387.
Keulen, N., Garde, A.A., Jorgart, T., 2015. Shock melting of K-feldspar and interlacing with cataclastically deformed plagioclase in granitic rocks at Toqqusap Nunaa, southern West Greenland: implications for the genesis of the Maniitsoq structure. Tectonophysics 662, 328–344.
Kirkland, C.L., Spaggiari, C.V., Pawley, M.J., Wingate, M.T.D., Smithies, R.H., Howard, H.M., Tyler, I.M., Belousova, E.A., Poujol, M., 2012. On the edge: U-Pb, Lu-Hf, and Sm-Nd data suggests reworking of the Yilgarn craton margin during formation of the Albany-Fraser Orogen. Precambrian Res. 187, 223–247.
Kirkland, C.L., Yalcymchuk, C., Hollis, J., Heide-Jorgensen, H., Danigik, M., 2018. Mesoarchean exhumation of the Akia terrane and a common Neoarchean tectonothermal history for West Greenland. Precambrian Res. 314, 129–144.
Kita, N.T., Ushikubo, T., Fu, B., Valley, J.W., 2009. High precision SIMS oxygen isotope analysis and the effect of sample topography. Chem. Geol. 264, 43–57.
Kring, D.A., 2000. Impact events and their effect on the origin, evolution, and distribution of life. GSA Today 10, 1–7.
Moser, D.E., Cupelli, C.L., Barker, I.R., Flowers, R.M., Bowman, J.R., Wooden, J., Hart, J.R., 2011. New zircon shock phenomena and their use for dating and reconstruction of large impact structures revealed by electron nanobeam (EBSD, CL, EDS) and isotopic U-Pb and (U-Th)/He analysis of the Vredefort dome. Can. J. Earth Sci. 48, 117–139.
Muttik, N., Kirsimaee, K., Vennemann, T.W., 2010. Stable isotope composition of smectite in suevites at the Ries crater, Germany: implications for hydrous alteration of impactites. Earth Planet. Sci. Lett. 299, 190–195.
Nasdala, L., Hanchar, J.M., Kronz, A., Whitehouse, M.J., 2005. Long-term stability of alpha particle damage in natural zircon. Chem. Geol. 220, 83–103.
Nutman, A.P., Friend, C.R.L., 2007. Adjacent terranes with ca. 2715 and 2650 Ma high-pressure metamorphic assemblages in the Nuuk region of the North Atlantic Craton, southern West Greenland: complexities of Neoarchaean collisional orogeny. Precambrian Res. 155, 159–203.
O'Neill, C., Marchi, S., Bottke, W., Fu, R., 2020. The role of impacts on Archaean tectonics. Geology 48, 174–178.
Osinski, G.R., Spray, J.G., Lee, P., 2001. Impact-induced hydrothermal activity within the Haughton impact structure, arctic Canada: generation of a transient, warm, wet oasis. Meteorit. Planet. Sci. 36, 731–745.
Osinski, G.R., Tornabene, L.L., Banerjee, N.R., Cockell, C.S., Flemming, R., Izawa, M.R.M., McCutcheon, J., Parnell, J., Preston, L.J., Pickersgill, A.E., Pontefract, A., Sapers, H.M., Southam, G., 2013. Impact-generated hydrothermal systems on Earth and Mars. Icarus 224, 347–363.
Piazolo, S., Austrheim, H., Whitehouse, M., 2012. Brittle-ductile microfabrics in naturally deformed zircon: deformation mechanisms and consequences for U-Pb dating. Am. Mineral. 97, 1544–1563.
Polat, A., Wang, L., Appel, P.W., 2015. A review of structural patterns and melting processes in the Archean craton of West Greenland: evidence for crustal growth at convergent plate margins as opposed to non-uniformitarian models. Tectonophysics 662, 67–94.
Reddy, S.M., Timms, N.E., Hamilton, P.J., Smyth, H.R., 2009. Deformation-related microstructures in magmatic zircon and implications for diffusion. Contrib. Mineral. Petrol. 157, 231–244.
Reimold, W.U., Gibson, R.L., Koeberl, C., 2013. Comment on "Searching for giant, ancient impact structures on Earth: the Mesoarchaean Maniitsoq structure, West Greenland" by Garde et al. [Earth Planet. Sci. Lett. 337–338 (2012) 197–210]. Earth Planet. Sci. Lett. 369, 333–335.
Riller, U., 2005. Structural characteristics of the Sudbury impact structure, Canada: impact-induced versus orogenic deformation—a review. Meteorit. Planet. Sci. 40, 1723–1740.
Rubatto, D., 2017. Zircon: the metamorphic mineral. Rev. Mineral. Geochem. 83, 261–295.
Scherstén, A., Garde, A.A., 2013. Complete hydrothermal re-equilibration of zircon in the Maniitsoq structure, West Greenland: a 3001 Ma minimum age of impact? Meteorit. Planet. Sci. 48, 1472–1498.
Schmieder, M., Kring, D.A., 2020. Earth's impact events through geologic time: a list of recommended ages for terrestrial impact structures and deposits. Astrobiology 20, 91–141.
Spencer, C.J., Cawood, P.A., Hawkesworth, C.J., Raub, T.D., Prave, A.R., Roberts, N.M., 2014. Proterozoic onset of crustal reworking and collisional tectonics: reappraisal of the zircon oxygen isotope record. Geology 42, 451–454.
Steenfelt, A., Hollis, J., Kirkland, C.L., Sandrin, A., Gardiner, N.J., Olierook, H.K.H., Szilas, K., Waterton, P., Yakymchuk, C., 2020. The Mesoarchaean Akia terrane, West Greenland, revisited: new insights based on spatial integration of geophysics, field observation, geochemistry and geochronology. Precambrian Res. 105958.
Szilas, K., Kelemen, P.B., Bernstein, S., 2015. Peridotite enclaves hosted by Mesoarchaean TTG-suite orthogneisses in the Fiskefjord region of southern West Greenland. GeoResJ 7, 22–34.
Timms, N.E., Erickson, T.M., Pearce, M.A., Cavosie, A.J., Schmieder, M., Tohver, E., Reddy, S.M., Zanetti, M.R., Nemchin, A.A., Wittmann, A., 2017. A pressure-temperature phase diagram for zircon at extreme conditions. Earth-Sci. Rev. 165, 185–202.
Valley, J.W., Lackey, J.S., Cavosie, A.J., Clechenko, C.C., Spicuzza, M.J., Basei, M., Bindeman, I.N., Ferreira, V.P., Sial, A.N., King, E.M., Peck, W.H., Sinha, A.K., Wei, C.S., 2005. 4.4 billion years of crustal maturation: oxygen isotope ratios of magmatic zircon. Contrib. Mineral. Petrol. 150, 561–580.
Van Kranendonk, M.J., Kirkland, C.L., Cliff, J., 2015. Oxygen isotopes in Pilbara Craton zircons support a global increase in crustal recycling at 32 Ga. Lithos 228, 90–98.
Wang, X., Coble, M.A., Valley, J.W., Shu, X., Kitajima, K., Spicuzza, M.J., Sun, T., 2014. Influence of radiation damage on Late Jurassic zircon from southern China: evidence from in situ measurements of oxygen isotopes, laser Raman, U–Pb ages, and trace elements. Chem. Geol. 389, 122–136.